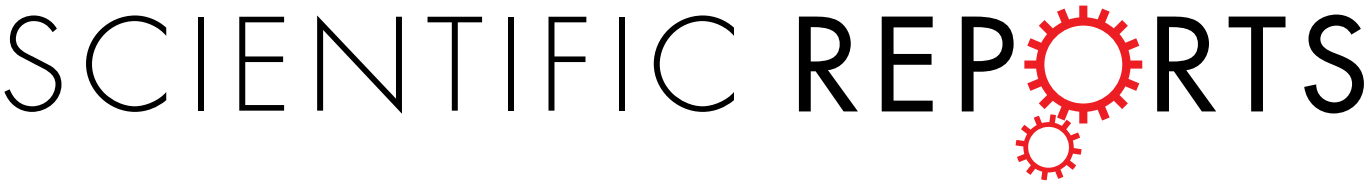

OPEN

S100B immunization triggers NFκB and complement activation in an autoimmune glaucoma model

Received: 1 September 2017
Accepted: 13 June 2018
Published online: 29 June 2018

Sabrina Reinehr[1], Jacqueline Reinhard[2], Marcel Gandej[1], Ivo Gottschalk[1], Gesa Stute[1], Andreas Faissner[2], H. Burkhard Dick[1] & Stephanie C. Joachim[1]

In glaucoma, latest studies revealed an involvement of the complement system with and without an elevated intraocular pressure. In the experimental autoimmune glaucoma model, immunization with antigens, such as S100B, lead to retinal ganglion cell (RGC) loss and optic nerve degeneration after 28 days. Here, we investigated the timeline of progression of the complement system, toll-like-receptor 4 (TLR4), and the transcription factor nucleus factor-kappa B (NFκB). Therefore, rats were immunized with S100B protein (S100) and analyzed at 3, 7, and 14 days. RGC numbers were comparable at all points in time, whereas a destruction of S100 optic nerves was noted at 14 days. A significant increase of mannose binding lectin (MBL) was observed in S100 retinas at 3 days. Subsequently, significantly more MBL$^+$ cells were seen in S100 optic nerves at 7 and 14 days. Accordingly, C3 was upregulated in S100 retinas at 14 days. An increase of interleukin-1 beta was noted in S100 aqueous humor samples at 7 days. In this study, activation of complement system via the lectin pathway was obvious. However, no TLR4 alterations were noted in S100 retinas and optic nerves. Interestingly, a significant NFκB increase was observed in S100 retinas at 7 and 14 days. We assume that NFκB activation might be triggered via MBL leading to glaucomatous damage.

Glaucoma is defined as a progressive optic neuropathy with changes at the optic nerve head, gradual retinal ganglion cell (RGC) death, and visual field loss[1]. An elevated intraocular pressure (IOP) is still considered the main risk factor[1], but there are increasing evidences that other pathological factors are involved. Some glaucoma patients, who do not have an elevated IOP, also show glaucomatous damage[2]. Glaucoma is a multifactorial disease and besides other factors recent studies revealed a contribution of immunological processes[3–5]. To analyze these mechanisms, the experimental autoimmune glaucoma model (EAG) was developed. Here, immunization with ocular antigens leads to RGC loss and optic nerve degeneration without IOP elevation[6–9]. In this model, autoreactive antibodies were detected in the retinas as well as in optic nerves[6,10]. Furthermore, an increase in microglia cell numbers, the macrophages of the central nervous system (CNS), was noted in these retinas and optic nerves[8,11]. This raises the question whether the microglia are an epiphenomenon or part of the degeneration process. For instance, retinal microglia can produce complement system proteins[12–14]. The complement system, as part of the innate immune system, is activated via three distinct routes. The classical pathway can be initiated through the protein C1q, while the mannose-binding-lectin (MBL) induces the lectin pathway. The alternative pathway is spontaneously activated through cleavage of C3b. All three ways are assembled in the terminal pathway, which starts with the protein C3. Finally, the membrane attack complex (MAC) forms a pore in the target cell and forces its lysis. In the last years, studies showed a contribution of the complement system in glaucoma disease, e.g. depositions of complement components were observed in the human glaucomatous retina[15,16]. Those depositions were also noted in ocular hypertension (OHT) animal models[17,18]. Our group could also show an IOP-independent activation of the complement system in retinas and optic nerves[19].

One regulator of the innate immune system is the transcription factor nucleus factor-kappa-light-chain-enhancer of activated B cells (NFκB). It controls several cellular mechanisms such as proliferation, differentiation, survival, and apoptosis[20]. In unstimulated cells, NFκB accumulates in the cytoplasm. After stimulation, the inhibitory protein IκBα dissociates from the NFκB complex and the transcription factor translocates into the nucleus

[1]Experimental Eye Research Institute, University Eye Hospital, Ruhr-University Bochum, In der Schornau 23-25, 44892, Bochum, Germany. [2]Department of Cell Morphology and Molecular Neurobiology, Faculty of Biology and Biotechnology, Ruhr-University Bochum, Universitaetsstrasse 150, 44780, Bochum, Germany. Correspondence and requests for materials should be addressed to S.C.J. (email: stephanie.joachim@rub.de)

	3 days	7 days	14 days
Bax/Bcl-2	0.99 (0.67–1.44)	0.89 (0.76–1.17)	0.84 (0.77–0.96)
P-value	0.9	0.4	0.07
C3	0.57 (0.20–1.16)	0.73 (0.53–1.07)	1.56 (1.33–1.87)
P-value	0.1	0.2	**<0.001**
C5	0.84 (0.50–1.31)	1.47 (1.06–1.98)	0.79 (0.62–0.96)
P-value	0.5	0.3	0.3
Factor B	2.22 (1.41–3.82)	0.76 (0.54–1.26)	0.54 (0.37–1.09)
P-value	**0.02**	0.3	0.3
Mbl	1.66 (1.31–2.22)	0.91 (0.73–1.09)	0.48 (0.32–0.839)
P-value	**0.047**	0.6	0.08
NEMO	0.76 (0.55–1.05)	1.00 (0.87–1.21)	0.93 (0.86–0.99)
P-value	0.09	0.99	0.2
Nfκb	0.83 (0.57–1.31)	1.33 (1.06–1.67)	0.97 (0.86–1.07)
P-value	0.4	0.2	0.8
Myd88	1.48 (0.99–2.44)	0.86 (0.72–1.13)	0.92 (0.75–1.29)
P-value	0.1	0.3	0.7
Pou4f1	0.80 (0.52–1.22)	1.16 (0.90–1.42)	0.94 (0.85–1.08)
P-value	0.3	0.3	0.4
Tlr4	1.04 (0.72–1.50)	1.45 (0.89–2.13)	1.11 (0.89–1.35)
P-value	0.8	0.4	0.5

Table 1. Analyses of mRNA levels via quantitative real-time PCR. Significant values are marked in bold.

to initiate the expression of various target genes[21,22]. Therefore, we analyze if NFκB activation can be initialized via toll-like-receptors (TLRs). This receptor family is located on microglia, dendritic cells, and macrophages[23,24]. TLR4 is known to play a role in neuronal cell death in the CNS[25]. Also, in glaucoma, an increased TLR4 expression seems to be involved in neurodegenerative processes. In human glaucoma donor eyes as well as in OHT animal models, an increase of TLRs was noted[26]. In optic nerve injury models, an activation of the TLR4/NFκB pathway was also observed[27,28].

We propose an activation of the complement system as well as an enhanced TLR4/NFκB pathway signaling in retinas and optic nerves of the EAG model before cell loss. To investigate this hypothesis, several cell types were evaluated via immunohistology and quantitative real-time PCR (qRT-PCR) 3, 7, and 14 days after immunization. Additionally, the levels of interleukin-1 beta (IL-1β) were measured in serum and aqueous humor samples at all points in time.

We did not find alterations in the number of RGCs, while an optic nerve degeneration was seen after 14 days in the S100 group. Furthermore, we detected an activation of the complement system through the lectin pathway after 3 days, while the expression of TLR4 was not affected at all investigated points in time. However, we noted an increased number of NFκB$^+$ cells in the S100 retinas. Additionally, an increase of IL-1β was observed in S100 aqueous humor samples at 7 days.

Results

No apoptotic retinal ganglion cells, but optic nerve degeneration. At 14 days, Brn-3a stained retinal whole mounts revealed no statistically significant alterations in the S100 group ($p > 0.05$, supplement Fig. 1A,B). However, in total as well as in the three separate regions of the whole mounts (central, middle, peripheral), a slight decline of about 10% of RGCs was observable. The number of RGCs on retinal cross-sections was comparable in S100 and Co animals at 3, 7, and 14 days ($p > 0.05$, supplement Fig. 1C,D). Also, no changes were observed in cleaved caspase$^+$ RGCs in the S100 group after all points in time ($p > 0.05$, supplement Fig. 1C,E). QRT-PCR revealed no alterations in the expression level of *Pou4f1* and *Bax/Bcl-2* ($p > 0.05$, supplement Fig. 1F,G, Table 1). In regard to SMI-32 labeling in the optic nerve, no changes occurred in the S100 group after 3 and 7 days ($p > 0.05$, Fig. 1A,B). However, a significantly higher SMI-32 score was noted in S100 animals at 14 days ($p = 0.007$). The S100B optic nerve staining showed no alterations between both groups throughout the study ($p > 0.05$, Fig. 1C,D).

Slight complement activation via the lectin pathway in retinas after immunization. For retinal C3, no changes were noted in the S100 group after 3 and 7 days ($p > 0.05$, Fig. 2A,B). Also, no alterations were seen in *C3* mRNA expression levels at these points in time ($p > 0.05$, Fig. 2C). At 14 days, significantly more C3$^+$ cells could be observed in the S100 animals ($p = 0.04$). Additionally, a significant upregulation of *C3* mRNA was detected at this point in time ($p < 0.001$, Table 1). C3 cell numbers on optic nerves were comparable in both groups throughout the study ($p > 0.05$, Fig. 2D,E).

In regard to retinal MAC expression, the immunohistological data revealed no alterations in the S100 group at all points in time ($p > 0.05$, supplement Fig. 2A,B). MAC was often co-localized with Brn-3a$^+$ cells (supplement Fig. 3). Also, the *C5* mRNA expression remained unaltered at 3, 7, and 14 days ($p > 0.05$, supplement Fig. 2C).

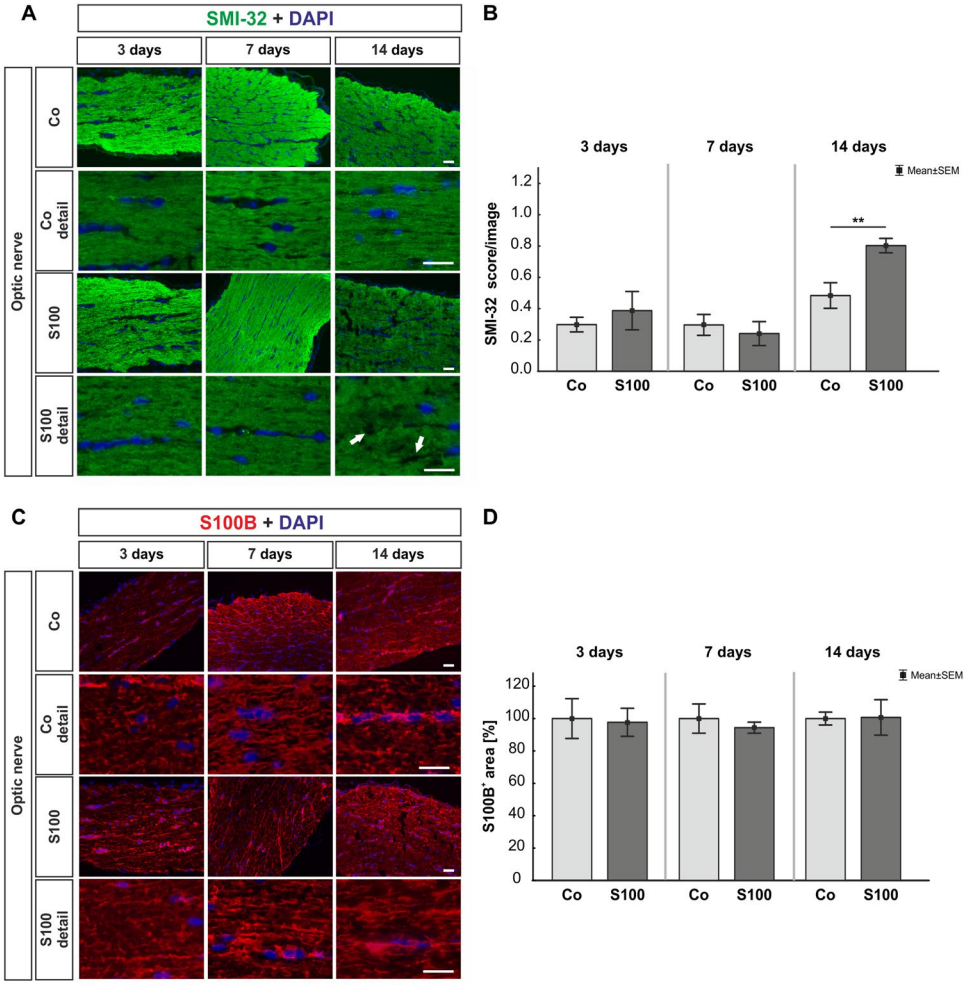

Figure 1. Optic nerve degeneration. **(A)** At 3, 7, and 14 days, neurofilaments were labeled with anti-SMI-32 (green). Cell nuclei were stained with DAPI (blue). Arrows point towards disrupted filaments. **(B)** No changes were noted in the SMI-32 score 3 and 7 days after immunization ($p > 0.05$). However, a significant increase of the SMI-32 score was observed in S100 optic nerves at 14 days ($p = 0.007$). **(C)** Astrocytes in the optic nerves were labeled with an anti-S100B antibody (red) and DAPI (blue). **(D)** We did not note any changes regarding the $S100B^+$ area in the S100 optic nerves compared to controls ($p > 0.05$). Values are mean ± SEM. Scale bars: 20 µm.

In the optic nerves, MAC staining was comparable in both groups at all points in time ($p > 0.05$, supplement Fig. 2D,E).

Regarding retinal factor B, no alterations were observed in the S100 animals at 3, 7, and 14 days ($p > 0.05$, Fig. 3A,B). Interestingly, an upregulation of *factor b* mRNA was noted in the S100 retinas at 3 days ($p = 0.02$, Fig. 3C, Table 1). At 7 and 14 days, the expression went back to control level ($p > 0.05$).

Significantly more MBL^+ cells were noted in the S100 retinas after 3 days ($p < 0.0001$, Fig. 3D,E). MBL was often co-localized with active microglia (supplement Fig. 3). Additionally, the qRT-PCR analysis revealed an upregulation of *Mbl* mRNA at this point in time ($p = 0.047$, Fig. 3F). At 7 days, the number of MBL^+ cells in both groups was similar ($p > 0.05$). This was still the case at 14 days ($p > 0.05$). No changes were observed regarding *Mbl* expression at 7 and 14 days ($p > 0.05$, Table 1). In the optic nerves, the number of MBL^+ cells remained unaltered after 3 days ($p > 0.05$, Fig. 3G,H). At 7 days, significantly more MBL^+ cells were observed in the S100 optic nerves ($p = 0.03$). An increased number of MBL^+ cells was still noted after 14 days ($p = 0.02$).

Increase of retinal NFκB. At 3 days, no changes were noted in regard to NFκB labeling in the S100 group ($p > 0.05$). More $NF\kappa B^+$ cells were observed after 7 days ($p = 0.03$). Also, a higher number of $NF\kappa B^+$ cells was revealed in the S100 retinas at 14 days ($p = 0.03$, Fig. 4A,B). The qRT-PCR data showed no alterations in *Nfκb* expression after 3 and 14 days ($p > 0.05$, Table 1), while a slight trend pointed towards an upregulation was noted at 7 days ($p = 0.18$, Fig. 4C). Furthermore, analyses of *Myd88* expression levels revealed a slight upregulation at 3 days ($p = 0.1$, Table 1). At 7 and 14 days, the expression of *Myd88* remained unaltered ($p > 0.05$, Fig. 4D). The mRNA expression levels of *NEMO* showed no changes at all points in time ($p > 0.05$, Fig. 4E, Table 1).

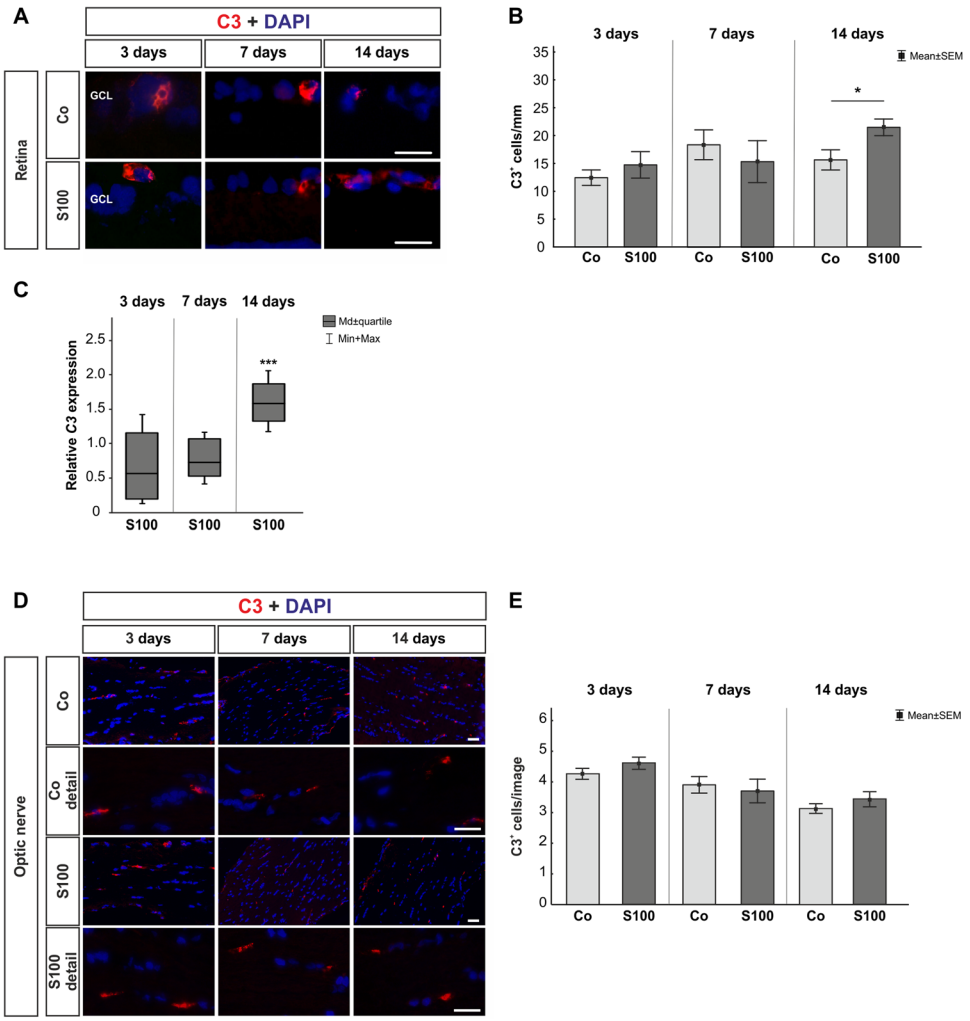

Figure 2. Mild C3 activation. **(A)** To evaluate an activation of C3, retinal cross-sections were stained with anti-C3 (red) and DAPI (cell nuclei, blue) 3, 7, and 14 after immunization. **(B)** No alterations in $C3^+$ cell numbers were noted in the S100 group after 3 and 7 days ($p > 0.05$). After 14 days, significantly more C3 depositions were observed ($p = 0.04$). **(C)** The *C3* mRNA expression level showed no alterations 3 and 7 days after immunization ($p > 0.05$). A significant higher level of *C3* mRNA was observed at 14 days ($p < 0.001$). **(D)** Anti-C3 staining (red) of the optic nerves was performed 3, 7, and 14 days after immunization. Cell nuclei were labeled with DAPI (blue). **(E)** No changes were revealed at all points in time ($p > 0.05$). Abbreviation: GCL = ganglion cell layer. Values are mean ± SEM for immunohistology and median ± quartile + maximum/minimum for qRT-PCR. Scale bars: 20 µm.

No TLR4 alterations in retinas and optic nerves. The analysis of $TLR4^+$ cells in the retinas showed no changes in the S100 group after 3, 7, and 14 days ($p > 0.05$, Fig. 5A,B). Also, the expression of *Tlr4* mRNA remained unaltered in the S100 retinas at all points in time ($p > 0.05$, Fig. 5C, Table 1). The quantification of $TLR4^+$ cells in the optic nerves also revealed no differences between both groups at all points in time ($p > 0.05$, Fig. 5D,E).

Enhanced levels of IL-1β in aqueous humor. ELISA analysis of IL-1β in sera of S100B animals revealed comparable levels as in control animals at all points in time ($p > 0.05$, Fig. 6A). Also, the concentration levels of IL-1β in the aqueous humor were comparable in both groups at 3 and 14 days ($p > 0.05$, Fig. 6B). Nevertheless, 7 days after immunization, a significantly higher concentration of IL-1β was measured in the aqueous humor of S100B animals ($p = 0.03$).

Discussion

Complement activation in glaucoma pathogenesis. Several studies indicate an involvement of the immune system in the pathogenesis of glaucoma. Besides findings of autoantibody patterns and depositions, also an activation of microglia was noted in both human glaucoma[4,5,29] and in experimental animal studies[8,11]. Therefore, a contribution of the complement system in glaucoma disease seems likely. In the study presented here, we noted an activation of the complement system via the lectin pathway, before any cell loss or optic nerve degeneration occurred. This is consistent with previous findings from our group, where the complement system was

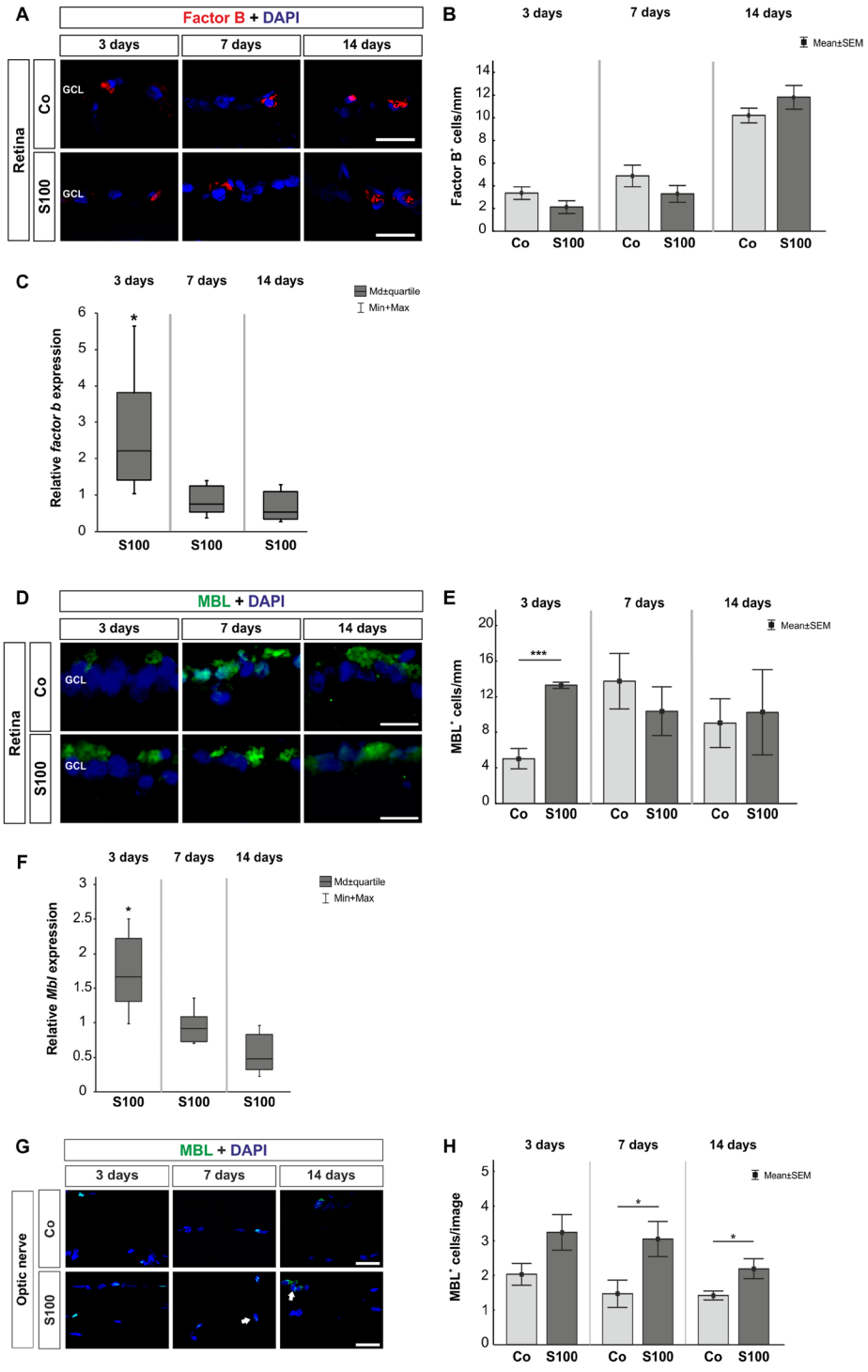

Figure 3. Activation through the lectin pathway. **(A)** Retinas were labeled with an antibody against factor B (red) 3, 7, and 14 days after immunization. Cell nuclei were stained with DAPI (blue). **(B)** No alterations in factor B^+ cell numbers were noted in S100 animals compared to controls at all points in time ($p > 0.05$). **(C)** The qRT-PCR analyses revealed an upregulation of *factor b* mRNA at 3 days ($p = 0.02$). No changes were observed at 7 and 14 days ($p > 0.05$). **(D)** Retinal cross-sections were stained with anti-MBL (green) and DAPI (blue) at 3, 7, and 14 days. **(E)** At 3 days, significantly more MBL^+ cells were observed in S100 retinas ($p < 0.0001$). No changes were noted later on ($p > 0.05$). **(F)** Expression levels of *Mbl* measured with qRT-PCR at 3, 7, and 14 days. At 3 days, a significant increase of *Mbl* mRNA expression was detected in S100 retinas ($p = 0.048$). *Mbl* went back to control level later on ($p > 0.05$). **(G)** Optic nerve sections were labeled with an anti-MBL antibody (green) and cell nuclei with DAPI (blue) 3, 7, and 14 days after immunization. **(H)** The number of MBL^+ cells remained unaltered in S100 optic nerves at 3 days ($p > 0.05$). After 7 days, significantly more MBL^+ cells were noted in the S100 group ($p = 0.03$) and were still present at 14 days ($p = 0.02$). Abbreviation: GCL = ganglion cell layer. Values are mean ± SEM for immunohistology and median ± quartile + maximum/minimum for qRT-PCR. Scale bars: 20 µm.

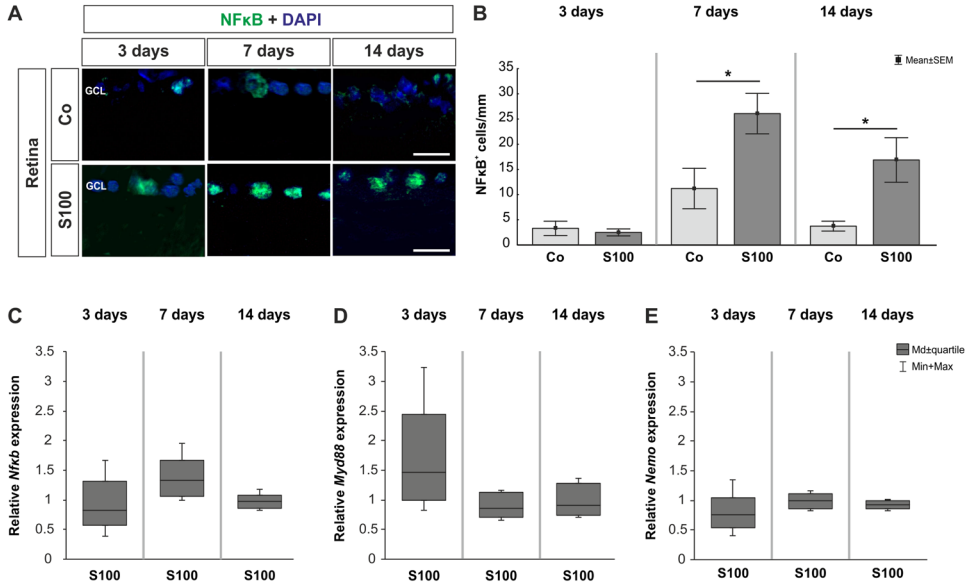

Figure 4. Increased NFκB staining. **(A)** Retinas were labeled with an anti-NFκB antibody (green) and DAPI (blue). **(B)** At 3 days, no changes were observed in regard of the number of NFκB$^+$ cells in the S100 group ($p > 0.05$). After 7 days, significantly more NFκB$^+$ cells were noted in S100 animals ($p = 0.03$). A significant increase of NFκB$^+$ cells was still revealed in this group after 14 days ($p = 0.03$). **(C)** QRT-PCR analysis revealed no differences in *Nfκb* mRNA expression at all points in time ($p > 0.05$). However, a slight trend towards an upregulation could be observed at 7 days ($p = 0.18$). **(D)** The expression levels of *Myd88* showed a trend towards an upregulation at 3 days ($p = 0.1$). At 7 and 14 days, no alterations were noted ($p > 0.05$). **(E)** At all points in time, the expression of *NEMO* mRNA remained unchanged ($p > 0.05$). Abbreviation: GCL = ganglion cell layer. Values are mean ± SEM for immunohistology and median ± quartile + maximum/minimum for qRT-PCR. Scale bars: 20 µm.

also initiated through the lectin route following immunization with an optic nerve homogenate antigen (ONA)[19]. MBL, an initiator of the lectin pathway, is a C-type lectin belonging to the collectins[30]. An increase of MBL$^+$ cells in the retina was observed at 3 days and an enhancement of NFκB at 7 and 14 days. Since collectins are able to trigger NFκB activation, it is possible that in this model NFκB is triggered via MBL, which subsequently might lead to cell death. Interestingly, in human glaucoma as well as in OHT models, the classical pathway was upregulated[17,31,32]. However, proteomic analysis of human glaucoma donor retinas also revealed an upregulation of proteins linked to the lectin pathway[15]. Additionally, we found a slight increase of the alternative pathway via qRT-PCR analyses. An inappropriate alternative pathway response is known to occur in eye diseases like age-related macular degeneration (AMD). Here, factor B related genes are upregulated, while factor H genes are downregulated[33]. Factor H is an inhibitor of the alternative pathway due to cleavage of C3 leading to its inactivation [34]. In animal models of AMD, an involvement of the lectin pathway is suggested[12,35,36]. These studies revealed that the alternative pathway is not only sufficient for injury in AMD, its initial activation is also triggered via the alternative and the lectin pathway. Due to the fact that both pathways are activated in our model, an interaction of those could be assumed. However, investigations of the alternative route in glaucoma are rare and need to be extended.

Enhanced NFκB signaling without TLR4 contribution. The transcription factor NFκB is constitutively expressed in the CNS and is activated in various neurological diseases, such as Morbus Alzheimer, Morbus Parkinson, or Huntington's disease[37–40]. It is known that components of NFκB are TLR induced genes that undergo positive feedback regulation by NFκB[41]. In human glaucomatous retinas, an upregulation of TLRs in microglia and astrocytes was reported[26]. It could also be observed that TLR4 signaling and NFκB activation accompanied by complement upregulation is a key mechanism of neuroinflammation[42]. An increase of NFκB was observed in the trabecular meshwork of glaucoma patients[43,44]. In microglia, NFκB controls migration to the site of injury due to expression of β-integrin CD11a. In our study, we noted an increase of NFκB in the retinas 7 and 14 days after immunization. This is followed by an activation of microglia at 14 days, which was previously described[8]. Furthermore, enhanced levels of the pro-inflammatory cytokine IL-1β were observed in S100 aqueous humor at 7 days. Yoneda *et al*. noted that IL-1β plays an important role in mediating ischemic and excitotoxic damage in glaucomatous retina[45]. Several studies indicate that IL-1β is secreted by microglia in photo-oxidative damage[46–48], neovascular AMD[49], retinitis pigmentosa[50], and retinal detachment[51]. But not only microglia/macrophages, also NFκB was found to play multiple roles in the induction of IL-1β transcription[52].

Regarding TLR4, we could not note any alterations in retinas and optic nerves in the EAG model throughout the study. Possibly, an upregulation of TLR4 could be observed at subsequent points in time, since a loss of RGCs is not measurable before day 28 in this model[7,8,19].

Nonetheless, these results strengthen the hypothesis that NFκB plays a crucial role in glaucoma pathogenesis.

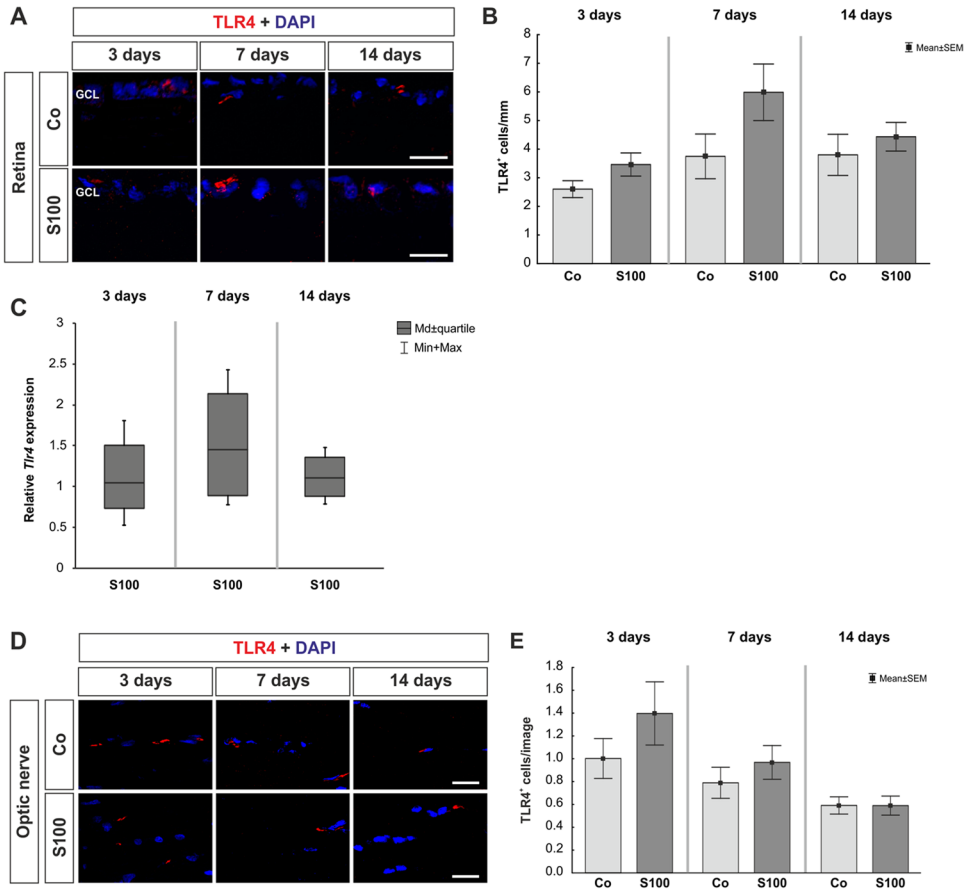

Figure 5. No TLR4 alterations in retina and optic nerve. **(A)** Retinal cross-sections were labeled with an anti-TLR4 antibody (red) and DAPI (blue) at 3, 7, and 14 days. **(B)** No alterations in the number of TLR4$^+$ cells were observed in the S100 retinas at all points in time ($p > 0.05$). **(C)** Also, no altered *Tlr4* mRNA expression could be noted at all points in time via qRT-PCR ($p > 0.05$). **(D)** To determine TLR4 expression in optic nerves, sections were stained with anti-TLR4 (red) and DAPI (cell nuclei, blue). **(E)** After 3 days, no changes were seen regarding the TLR4 expression in the S100 animals ($p > 0.05$). Also, no alterations were detected later on ($p > 0.05$). Abbreviation: GCL = ganglion cell layer. Values are mean ± SEM for immunohistology and median ± quartile + maximum/minimum for qRT-PCR. Scale bars: 20 µm.

Conclusion

We conclude that the early activation via the lectin complement pathway triggers NFκB signaling with subsequent microglia response in this EAG model. The combination of these mechanisms seems to initiate the IOP-independent RGC death and optic nerve degeneration. Therefore, an inhibition of complement components might lead to protection of RGCs and optic nerve fibers. However, further studies are required to gain more knowledge regarding the interaction of NFκB/complement signaling components and their contribution to glaucoma like RGC death.

Methods

Animals. All procedures concerning animals adhered to the ARVO statement for the use of animals in ophthalmic and vision research. All experiments involving animals were approved by the animal care committee of North Rhine-Westphalia, Germany, and were performed in accordance with relevant guidelines and regulations.

Male Lewis rats (Charles River, Sulzfeld, Germany), 6 weeks of age, were used for the experiments and kept under environmentally controlled conditions with free access to chow and water. Detailed observations and health checks, including eye exams, were performed regularly, as described previously[53].

Immunizations. Rats received 1 mg/ml S100B (Sigma Aldrich, Munich, Germany)[7,8]. The antigen was mixed with incomplete Freund's adjuvant (200 µl) plus 3 µg pertussis toxin (both Sigma Aldrich). The animals of the control group (Co) were injected with 0.9% NaCl in Freund's adjuvant and pertussis toxin.

For tissue dissection, animals were sacrificed with an overdose CO_2 at 3, 7, and 14 days after immunization.

Retinal ganglion cell counts via whole mounts. 14 days after immunization, eyes were fixed in 4% paraformaldehyde (PFA) for one hour and then prepared as whole mounts (n = 6/group)[19]. The following steps

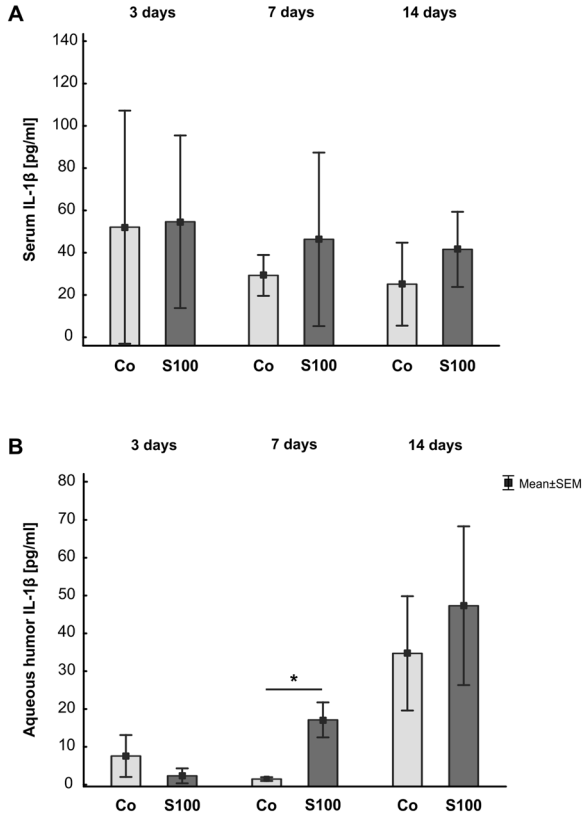

Figure 6. Increased IL-1β levels in aqueous humor. **(A)** The concentration level of IL-1β was measured in rat serum at 3, 7, and 14 days after immunization. The levels of IL-1β were comparable in both groups at all points in time. **(B)** IL-1β was also analyzed in aqueous humor 3, 7, and 14 days after immunization. While no changes were noted at 3 days ($p > 0.05$), a significant increase of IL-1β could be observed in the S100 group after 7 days ($p = 0.03$). At 14 days, the IL-1β concentration level was comparable in both groups. Values are mean ± SEM.

were performed at 20 °C on a thermo shaker (70 rpm). First, the whole mounts were blocked with 10% donkey serum and 0.5% Triton-X in PBS for 90 min. Then, they were incubated with the RGC marker Brn-3a[54] (1:300; Santa Cruz, CA, USA) overnight, followed by a 2 hour incubation of donkey anti-goat Alexa Flour 488 (1:1000; Dianova, Hamburg, Germany). From each of the four whole mount arms, three photos were captured (central, middle, and peripheral) with an Axiocam HRc CCD camera on an Axio Imager M1 fluorescence microscope (Zeiss, Jena, Germany). Cells were counted using ImageJ software (V 1.43 u; NIH, Bethesda, MD, USA).

Retina and optic nerve histology. Retinas and optic nerves were fixed in 4% PFA for 1 (retina) or 2 hours (optic nerves), dehydrated in sucrose, and embedded in Tissue Tek (Thermo Fisher, Waltham, CA, USA). Cross-sections of the retina (10 µm) and longitudinal optic nerve sections (4 µm) were cut with a Cryostat (Thermo Fisher) and mounted on Superfrost slides (Thermo Fisher).

Immunohistology of retinal and optic nerve sections. To identify the different cell types in the retina and the optic nerve, specific immunofluorescence antibodies were applied (retina: n = 5–6/group, optic nerve: n = 6–8/group, 6 sections/staining; Table 2)[19]. Briefly, retina and optic nerve sections were blocked with a solution containing 10–20% donkey and/or goat serum and 0.1% Triton-X in PBS. Primary antibodies were incubated at room temperature overnight. Incubation using corresponding secondary antibodies was performed for 1 h on the next day. Nuclear staining with 4′, 6 diamidino-2-phenylindole (DAPI) was included to facilitate the orientation on the slides. Negative controls were performed by using secondary antibodies only.

Histological examination of retinas and optic nerves. All photographs were taken with a fluorescence microscope (Axio Imager M1). In the retina, two photos of the peripheral and two of the central part of each section were captured for each point in time. In the optic nerve, three photos were captured (proximal, middle, and distal). The images were transferred to Corel Paint Shop Pro (V13, Corel Corporation, CA, USA) and equal excerpts were cut out. RGCs, cleaved caspase 3^+ RGCs, complement factors, $NF\kappa B^+$, and $TLR4^+$ cells were counted using ImageJ software. The neurofilament marker SMI-32 was evaluated via a scoring system ranging from 0 (intact structure) to 2 (loss of structural integrity, fissures, many retraction bulbs)[8,55,56]. Measurement and analysis of S100B area was performed using ImageJ software as described previously[53,57,58]. Briefly, images were transformed into grayscale. To minimize interference with background labeling, a rolling ball radius of 50 pixels was subtracted. Then, for each picture, a suitable lower threshold was set. The ideal threshold was obtained when

Primary antibodies				Secondary antibodies			
Antibody	**Company**	**Tissue**	**Dilution**	**Antibody**	**Company**	**Tissue**	**Dilution**
Anti-Brn-3a	SySy	Retina	1:1000	Donkey anti-rabbit Alexa Fluor 488	Invitrogen	Retina	1:500
Anti-Brn-3a	Santa-Cruz	Retina	1:100	Goat anti-mouse Alexa Fluor 488	Invitrogen	Retina	1:500
Anti-C3	Cedarlane	Retina	1:500	Goat anti-rabbit IgG Cy3	Linaris	Retina	1:500
		Optic nerve	1:500			Optic nerve	1:500
Anti-C5b-9 (MAC)	Biozol	Retina	1:100	Donkey anti-mouse DyLight 488	Dianova	Retina	1:250
		Optic nerve	1:100	Goat anti-mouse Alexa Fluor 488	Invitrogen	Optic nerve	1:500
Anti-cleaved caspase 3	Sigma-Aldrich	Retina	1:300	Donkey anti-rabbit Alexa Fluor 555	Invitrogen	Retina	1:500
Anti-ED1	Millipore	Retina	1:250	Donkey anti-mouse Alexa Fluor 488	Invitrogen	Retina	1:500
Anti-factor B	TECOmedical	Retina	1:1000	Donkey anti-goat Cy3	Abcam	Retina	1:600
Anti-MBL	Biozol	Retina	1:100	Donkey anti-rabbit Alexa Fluor 555	Invitrogen	Retina	1:500
				Goat anti-rabbit Alexa Fluor 488		Retina	1:600
		Optic nerve	1:100	Goat anti-rabbit Alexa Fluor 488		Optic nerve	1:600
Anti-NeuN	Millipore	Retina	1:500	Donkey anti-chicken Alexa Fluor 488	Jackson ImmunoResearch	Retina	1:500
Anti-NFκB p50	Santa-Cruz	Retina	1:500	Goat anti-mouse Alexa Fluor 488	Invitrogen	Retina	1:600
				Donkey anti-mouse Alexa Fluor 555			1:500
Anti-S100B	Novus Biological	Optic nerve	1:100	Donkey anti-rabbit Alexa Fluor 555	Invitrogen	Optic nerve	1:500
Anti-SMI-32	Biolegend	Optic nerve	1:2000	Goat anti-mouse Alexa Fluor 488	Invitrogen	Optic nerve	1:400
Anti-TLR4	Abcam	Retina	1:400	Donkey anti-rabbit Alexa Fluor 555	Invitrogen	Retina	1:500

Table 2. Primary and secondary antibodies used for immunohistochemistry.

Gene	Forward (F) and reverse (R) oligonucleotides	GenBank acc. no.	Amplicon size
Bax-F	gctggacactggacttcctc	NM_017059.2	127 bp
Bax-R	actccagccacaaagatggt		
Bcl-2-F	gtacctgaaccggcatctg	NM_016993.1	76 bp
Bcl-2-R	ggggccatatagttccacaa		
C3-F	tcgaaatccctcccaagtc	NM_016994.2	60 bp
C3-R	cgatcttcaaggggacaatg		
C5-F	tctcaggccaaagagagacc	XM001079130.4	73 bp
C5-R	acggtgtttgtatttagcagctt		
Cyclophilin-F	tgctggaccaaacacaaatg	M19553.1	88 bp
Cyclophilin-R	cttcccaaagaccacatgct		
Factor b-F	aagaaggcagaatgcagagc	NM_212466.3	66 bp
Factor b-R	ccagaactccccattttcaa		
Mbl-F	aggaccaaaaggccaaaaag	NM_012599.2	68 bp
Mbl-R	ccatatttgccagcttcacc		
Myd88-F	atgaactgaaggaccgcatc	XM_006244087.3	127 bp
Myd88-R	cccagttcctttgtctgtgg		
NEMO-F	tctgaagaaatgccaacagc	AY392762.1	61 bp
NEMO-R	tgtcacctgagctttcacaga		
Nfκb-F	ctggcagctcttctcaaagc	NM_001276711.1	70 bp
Nfκb-R	ccaggtcatagagaggctcaa		
Pou4f1-F	ctccggaccttgagcttct	XM_008770931.2	60 bp
Pou4f1-R	tagaagggagagttaaacacagaaca		
Tlr4-F	ccttgagaaagtggagaagtcc	NM_019178.1	61 bp
Tlr4-R	gctaagaaggcgatacaattcg		
β-actin-F	cccgcgagtacaaccttct	NM_031144.3	72 bp
β-actin-R	cgtcatccatggcgaact		

Table 3. Oligonucleotide sequences. The listed oligonucleotide pairs were used in quantitative real-time PCR experiments, while *β-actin* and *cyclophilin* served as housekeeping genes. The predicted amplicon sizes are given. Abbreviations: F = forward, R = reverse, acc. no. = accession number, bp = base pair.

the grayscale picture and the original one corresponded. Afterwards, the mean value of the lower threshold was calculated, and this number was used for final analysis. The percentage of the labeled area was measured between these defined thresholds: lower threshold: 11.61; upper threshold: 247.44.

RNA preparation and cDNA synthesis. For RNA preparation, retinas from every point in time were isolated, transferred into lysis buffer containing 2-mercaptoethanol (Sigma-Aldrich), and snap frozen in liquid nitrogen (n = 3–6/group). Total RNA was extracted with the Gene Elute Mammalian Total RNA Miniprep Kit according to the manufacturer's instructions (Sigma-Aldrich) and digested with RNase-free DNase I (Sigma-Aldrich). Quality and quantity of RNA were assessed by measuring the ratio of absorbance values at 260 and 280 nm (BioSpectrometer®, Eppendorf, Hamburg, Germany). Total RNA (1 µg) was used for reverse transcription with a cDNA synthesis kit (Thermo Fisher Scientific, Waltham, MA, USA).

Quantitative real-time PCR. The designed oligonucleotides are shown in Table 3. Real-time-PCR (Roche Applied Science, Mannheim, Germany) analyses were performed using SYBR Green I and the Light Cycler® 96 (Roche Applied Science)[19,59,60]. Oligonucleotide concentration was optimized to a final concentration of 200 nM and combined with 200 ng retinal cDNA per well. We set up two reactions per RNA sample (duplicates) with a final volume of 20 µl per single reaction[61–63]. Each qRT-PCR was performed in duplicates from each retina and for each point in time and repeated twice (n = 3–6/group). The average threshold cycle (Ct) values of the two independent experiments were used to calculate the ratios for the target genes[64]. In order to obtain amplification efficiencies of different primer sets, we generated standard curves by a twofold dilution series with template amounts ranging from 5 to 125 ng cDNA per well. The Ct values of two reference genes (*β-actin* and *cyclophilin*) were taken into account.

Measurement of IL-1β in serum and aqueous humor. Levels of the pro-inflammatory cytokine IL-1β in serum (n = 7/group) and aqueous humor (n = 4–6/group) were measured using a commercially available enzyme immunoassay kit 3, 7, and 14 days after immunization (ELISA; R&D systems, MN, USA). All samples were used undiluted. Each assay was performed according to the manufacturer's instruction. All measurements were performed on a microplate reader (AESKU Reader with Gen5 ELISA software, AESKU.DIAGNOSTICS, Wendelsheim, Germany)[65].

Statistics. Immunohistological and ELISA data are presented as mean ± SEM. The S100 group was compared to the Co group via two-tailed Student's t-test using Statistica Software (Version 13, Dell, Tulsa, OK, USA). Regarding qRT-PCR, data are presented as median ± quartile + minimum/maximum and were assessed using REST© software (Qiagen, Hilden, Germany)[64]. P-values below 0.05 were considered statistically significant. *$p < 0.05$, **$p < 0.01$, ***$p < 0.001$.

References

1. EGS. Terminology and guidelines for glaucoma. 4th Edition (2014).
2. Sommer, A. *et al*. Relationship between intraocular pressure and primary open angle glaucoma among white and black Americans. The Baltimore Eye Survey. *Arch Ophthalmol* **109**, 1090–1095 (1991).
3. Joachim, S. C., Pfeiffer, N. & Grus, F. H. Autoantibodies in patients with glaucoma: a comparison of IgG serum antibodies against retinal, optic nerve, and optic nerve head antigens. *Graefes Arch Clin Exp Ophthalmol* **243**, 817–823 (2005).
4. Grus, F. H., Joachim, S. C., Hoffmann, E. M. & Pfeiffer, N. Complex autoantibody repertoires in patients with glaucoma. *Mol Vis* **10**, 132–137 (2004).
5. Wax, M. B., Yang, J. & Tezel, G. Serum autoantibodies in patients with glaucoma. *J Glaucoma* **10**, S22–24 (2001).
6. Laspas, P. *et al*. Autoreactive antibodies and loss of retinal ganglion cells in rats induced by immunization with ocular antigens. *Invest Ophthalmol Vis Sci* **52**, 8835–8848 (2011).
7. Casola, C. *et al*. S100 Alone Has the Same Destructive Effect on Retinal Ganglion Cells as in Combination with HSP 27 in an Autoimmune Glaucoma Model. *J Mol Neurosci* **56**, 228–236 (2015).
8. Noristani, R. *et al*. Retinal and Optic Nerve Damage is Associated with Early Glial Responses in an Experimental Autoimmune Glaucoma Model. *J Mol Neurosci* **58**, 470–482 (2016).
9. Wax, M. B. *et al*. Induced autoimmunity to heat shock proteins elicits glaucomatous loss of retinal ganglion cell neurons via activated T-cell-derived fas-ligand. *J Neurosci* **28**, 12085–12096 (2008).
10. Joachim, S. C. *et al*. Immune response against ocular tissues after immunization with optic nerve antigens in a model of autoimmune glaucoma. *Mol Vis* **19**, 1804–1814 (2013).
11. Joachim, S. C. *et al*. Retinal ganglion cell loss is accompanied by antibody depositions and increased levels of microglia after immunization with retinal antigens. *Plos One* **7**, e40616 (2012).
12. Rutar, M. *et al*. Analysis of complement expression in light-induced retinal degeneration: synthesis and deposition of C3 by microglia/macrophages is associated with focal photoreceptor degeneration. *Invest Ophthalmol Vis Sci* **52**, 5347–5358 (2011).
13. Natoli, R. *et al*. Retinal Macrophages Synthesize C3 and Activate Complement in AMD and in Models of Focal Retinal Degeneration. *Invest Ophthalmol Vis Sci* **58**, 2977–2990 (2017).
14. Luo, C., Chen, M. & Xu, H. Complement gene expression and regulation in mouse retina and retinal pigment epithelium/choroid. *Mol Vis* **17**, 1588–1597 (2011).
15. Tezel, G. *et al*. Oxidative stress and the regulation of complement activation in human glaucoma. *Invest Ophthalmol Vis Sci* **51**, 5071–5082 (2010).
16. Boehm, N., Beck, S., Lossbrand, U., Pfeiffer, N. & Grus, F. H. Analysis of Complement Proteins in Retina and Sera of Glaucoma Patients. *Invest. Ophthalmol. Vis. Sci.* **51**, 5221 (2010).
17. Kuehn, M. H. *et al*. Retinal synthesis and deposition of complement components induced by ocular hypertension. *Exp Eye Res* **83**, 620–628 (2006).
18. Becker, S., Reinehr, S., Burkhard Dick, H. & Joachim, S. C. [Complement activation after induction of ocular hypertension in an animal model]. *Ophthalmologe* **112**, 41–48 (2015).
19. Reinehr, S. *et al*. Simultaneous Complement Response via Lectin Pathway in Retina and Optic Nerve in an Experimental Autoimmune Glaucoma Model. *Front Cell Neurosci* **10**, 140 (2016).
20. Gilmore, T. D. Introduction to NF-kappaB: players, pathways, perspectives. *Oncogene* **25**, 6680–6684 (2006).

21. Ghosh, S., May, M. J. & Kopp, E. B. NF-kappa B and Rel proteins: evolutionarily conserved mediators of immune responses. *Annu Rev Immunol* **16**, 225–260 (1998).
22. Fraser, D. A., Arora, M., Bohlson, S. S., Lozano, E. & Tenner, A. J. Generation of inhibitory NFkappaB complexes and phosphorylated cAMP response element-binding protein correlates with the anti-inflammatory activity of complement protein C1q in human monocytes. *J Biol Chem* **282**, 7360–7367 (2007).
23. Olson, J. K. & Miller, S. D. Microglia initiate central nervous system innate and adaptive immune responses through multiple TLRs. *J Immunol* **173**, 3916–3924 (2004).
24. Lehnardt, S. Innate immunity and neuroinflammation in the CNS: the role of microglia in Toll-like receptor-mediated neuronal injury. *Glia* **58**, 253–263 (2010).
25. Lehnardt, S. *et al*. Activation of innate immunity in the CNS triggers neurodegeneration through a Toll-like receptor 4-dependent pathway. *Proc Natl Acad Sci USA* **100**, 8514–8519 (2003).
26. Luo, C. *et al*. Glaucomatous tissue stress and the regulation of immune response through glial Toll-like receptor signaling. *Invest Ophthalmol Vis Sci* **51**, 5697–5707 (2010).
27. Lin, S. *et al*. Microglial TIR-domain-containing adapter-inducing interferon-beta (TRIF) deficiency promotes retinal ganglion cell survival and axon regeneration via nuclear factor-kappaB. *J Neuroinflammation* **9**, 39 (2012).
28. Halder, S. K., Matsunaga, H., Ishii, K. J. & Ueda, H. Prothymosin-alpha preconditioning activates TLR4-TRIF signaling to induce protection of ischemic retina. *Journal of neurochemistry* **135**, 1161–1177 (2015).
29. Gramlich, O. W. *et al*. Enhanced insight into the autoimmune component of glaucoma: IgG autoantibody accumulation and pro-inflammatory conditions in human glaucomatous retina. *PLoS One* **8**, e57557 (2013).
30. Holmskov, U., Thiel, S. & Jensenius, J. C. Collections and ficolins: humoral lectins of the innate immune defense. *Annu Rev Immunol* **21**, 547–578 (2003).
31. Stasi, K. *et al*. Complement component 1Q (C1Q) upregulation in retina of murine, primate, and human glaucomatous eyes. *Invest Ophthalmol Vis Sci* **47**, 1024–1029 (2006).
32. Howell, G. R. *et al*. Molecular clustering identifies complement and endothelin induction as early events in a mouse model of glaucoma. *J Clin Invest* **121**, 1429–1444 (2011).
33. Buentello-Volante, B. *et al*. Susceptibility to advanced age-related macular degeneration and alleles of complement factor H, complement factor B, complement component 2, complement component 3, and age-related maculopathy susceptibility 2 genes in a Mexican population. *Mol Vis* **18**, 2518–2525 (2012).
34. Weiler, J. M., Daha, M. R., Austen, K. F. & Fearon, D. T. Control of the amplification convertase of complement by the plasma protein beta1H. *Proc Natl Acad Sci USA* **73**, 3268–3272 (1976).
35. Rohrer, B. *et al*. The alternative pathway is required, but not alone sufficient, for retinal pathology in mouse laser-induced choroidal neovascularization. *Mol Immunol* **48**, e1–8 (2011).
36. Joseph, K. *et al*. Oxidative stress sensitizes retinal pigmented epithelial (RPE) cells to complement-mediated injury in a natural antibody-, lectin pathway-, and phospholipid epitope-dependent manner. *J Biol Chem* **288**, 12753–12765 (2013).
37. Kaltschmidt, B., Uherek, M., Volk, B., Baeuerle, P. A. & Kaltschmidt, C. Transcription factor NF-kappaB is activated in primary neurons by amyloid beta peptides and in neurons surrounding early plaques from patients with Alzheimer disease. *Proc Natl Acad Sci USA* **94**, 2642–2647 (1997).
38. Memet, S. NF-kappaB functions in the nervous system: from development to disease. *Biochem Pharmacol* **72**, 1180–1195 (2006).
39. Hunot, S. *et al*. Nuclear translocation of NF-kappaB is increased in dopaminergic neurons of patients with parkinson disease. *Proc Natl Acad Sci USA* **94**, 7531–7536 (1997).
40. Khoshnan, A. *et al*. Activation of the IkappaB kinase complex and nuclear factor-kappaB contributes to mutant huntingtin neurotoxicity. *J Neurosci* **24**, 7999–8008 (2004).
41. Takeuchi, O. & Akira, S. Pattern recognition receptors and inflammation. *Cell* **140**, 805–820 (2010).
42. Li, X., Long, J., He, T., Belshaw, R. & Scott, J. Integrated genomic approaches identify major pathways and upstream regulators in late onset Alzheimer's disease. *Sci Rep* **5**, 12393 (2015).
43. Wang, N., Chintala, S. K., Fini, M. E. & Schuman, J. S. Activation of a tissue-specific stress response in the aqueous outflow pathway of the eye defines the glaucoma disease phenotype. *Nat Med* **7**, 304–309 (2001).
44. Zhou, L., Li, Y. & Yue, B. Y. Oxidative stress affects cytoskeletal structure and cell-matrix interactions in cells from an ocular tissue: the trabecular meshwork. *J Cell Physiol* **180**, 182–189 (1999).
45. Yoneda, S. *et al*. Interleukin-1beta mediates ischemic injury in the rat retina. *Exp Eye Res* **73**, 661–667 (2001).
46. Jiao, H., Natoli, R., Valter, K., Provis, J. M. & Rutar, M. Spatiotemporal Cadence of Macrophage Polarisation in a Model of Light-Induced Retinal Degeneration. *PLoS One* **10**, e0143952 (2015).
47. Natoli, R. *et al*. Microglia-derived IL-1beta promotes chemokine expression by Muller cells and RPE in focal retinal degeneration. *Mol Neurodegener* **12**, 31 (2017).
48. Hu, S. J. *et al*. Upregulation of P2RX7 in Cx3cr1-Deficient Mononuclear Phagocytes Leads to Increased Interleukin-1beta Secretion and Photoreceptor Neurodegeneration. *J Neurosci* **35**, 6987–6996 (2015).
49. Lavalette, S. *et al*. Interleukin-1beta inhibition prevents choroidal neovascularization and does not exacerbate photoreceptor degeneration. *Am J Pathol* **178**, 2416–2423 (2011).
50. Zhao, L. *et al*. Microglial phagocytosis of living photoreceptors contributes to inherited retinal degeneration. *EMBO Mol Med* **7**, 1179–1197 (2015).
51. Kataoka, K. *et al*. Macrophage- and RIP3-dependent inflammasome activation exacerbates retinal detachment-induced photoreceptor cell death. *Cell Death Dis* **6**, e1731 (2015).
52. Cogswell, J. P. *et al*. NF-kappa B regulates IL-1 beta transcription through a consensus NF-kappa B binding site and a nonconsensus CRE-like site. *J Immunol* **153**, 712–723 (1994).
53. Casola, C. *et al*. Specific Inner Retinal Layer Cell Damage in an Autoimmune Glaucoma Model Is Induced by GDNF With or Without HSP27. *Invest Ophthalmol Vis Sci* **57**, 3626–3639 (2016).
54. Nadal-Nicolas, F. M. *et al*. Brn3a as a marker of retinal ganglion cells: qualitative and quantitative time course studies in naive and optic nerve-injured retinas. *Invest Ophthalmol Vis Sci* **50**, 3860–3868 (2009).
55. Wang, J., Hamm, R. J. & Povlishock, J. T. Traumatic axonal injury in the optic nerve: evidence for axonal swelling, disconnection, dieback, and reorganization. *J Neurotrauma* **28**, 1185–1198 (2011).
56. Schlamp, C. L., Li, Y., Dietz, J. A., Janssen, K. T. & Nickells, R. W. Progressive ganglion cell loss and optic nerve degeneration in DBA/2J mice is variable and asymmetric. *BMC Neurosci* **7**, 66 (2006).
57. Horstmann, L. *et al*. Inflammatory demyelination induces glia alterations and ganglion cell loss in the retina of anexperimental autoimmune encephalomyelitis model. *J Neuroinflammation* **10**, 120 (2013).
58. Reinehr, S. *et al*. HSP27 immunization reinforces AII amacrine cell and synapse damage induced by S100 in an autoimmune glaucoma model. *Cell Tissue Res*(2017).
59. Reinhard, J. *et al*. Ischemic injury leads to extracellular matrix alterations in retina and optic nerve. *Sci Rep* **7**, 43470 (2017).
60. Reinehr, S. *et al*. Early remodelling of the extracellular matrix proteins tenascin-C and phosphacan in retina and optic nerve of an experimental autoimmune glaucoma model. *J Cell Mol Med* **20**, 2122–2137 (2016).
61. Ray, A., Zoidl, G., Weickert, S., Wahle, P. & Dermietzel, R. Site-specific and developmental expression of pannexin1 in the mouse nervous system. *Eur J Neurosci* **21**, 3277–3290 (2005).

62. Horvat-Brocker, A. *et al*. Receptor protein tyrosine phosphatases are expressed by cycling retinal progenitor cells and involved in neuronal development of mouse retina. *Neuroscience* **152**, 618–645 (2008).
63. Luft, V., Reinhard, J., Shibuya, M., Fischer, K. D. & Faissner, A. The guanine nucleotide exchange factor Vav3 regulates differentiation of progenitor cells in the developing mouse retina. *Cell Tissue Res* (2014).
64. Pfaffl, M. W., Horgan, G. W. & Dempfle, L. Relative expression software tool (REST) for group-wise comparison and statistical analysis of relative expression results in real-time PCR. *Nucleic Acids Res* **30**, e36 (2002).
65. Tsai, T. *et al*. Anti-inflammatory cytokine and angiogenic factors levels in vitreous samples of diabetic retinopathy patients. *PLoS One* **13**, e0194603 (2018).

Acknowledgements
This work was supported by the Deutsche Forschungsgemeinschaft (DFG, grant JO-886/1-3). We acknowledge support by the DFG Open Access Publication Funds of the Ruhr-University Bochum.

Author Contributions
S.R. performed experiments, analyzed data and wrote the manuscript, J.R. analyzed data and revised the manuscript, M.G. and I.G. performed experiments and analyzed data, G.S. performed experiments, A.F. and H.B.D. revised the manuscript, S.C.J. designed the study and revised the manuscript. All authors have approved the final article.

Additional Information
Supplementary information accompanies this paper at https://doi.org/10.1038/s41598-018-28183-6.

Competing Interests: The authors declare no competing interests.

Publisher's note: Springer Nature remains neutral with regard to jurisdictional claims in published maps and institutional affiliations.

Open Access This article is licensed under a Creative Commons Attribution 4.0 International License, which permits use, sharing, adaptation, distribution and reproduction in any medium or format, as long as you give appropriate credit to the original author(s) and the source, provide a link to the Creative Commons license, and indicate if changes were made. The images or other third party material in this article are included in the article's Creative Commons license, unless indicated otherwise in a credit line to the material. If material is not included in the article's Creative Commons license and your intended use is not permitted by statutory regulation or exceeds the permitted use, you will need to obtain permission directly from the copyright holder. To view a copy of this license, visit http://creativecommons.org/licenses/by/4.0/.

© The Author(s) 2018